Cross-relaxation and ion clustering in Tm3+:CaF2 crystals

Pavel Loiko, A. Braud, Lauren Guillemot, Jean-Louis Doualan, Abdelmjid Benayad, Patrice Camy

Cross-relaxation and ion clustering in Tm^{3+}:CaF_2 crystals

Pavel Loiko[a,*], Alain Braud[a], Lauren Guillemot[a], Jean-Louis Doualan[a], Abdelmjid Benayad[a], and Patrice Camy[a]

[a]Centre de recherche sur les Ions, les Matériaux et la Photonique (CIMAP), UMR 6252 CEA-CNRS-ENSICAEN, Université de Caen, 6 Boulevard du Maréchal Juin, 14050 Caen, France

ABSTRACT

We systematically study cross-relaxation (CR) and ion clustering in Tm^{3+}:CaF_2 crystals using a spectroscopic approach. For this, the luminescence from the $^3H_4$ and $^3F_4$ states was monitored for a broad range of Tm^{3+} doping concentrations, from 0.01 at.% to 7 at.%. The decay curves were fitted using a model of two ions classes, namely isolated ions showing no energy-transfer processes and ions with neighbors exhibiting both CR and energy-transfer upconversion (ETU), and accounting for energy-migration. The fraction of ions with neighbors and the microscopic concentration-independent CR and ETU parameters are deduced. The critical Tm^{3+} doping level for which at least half of the active ions are clustered is only 0.7 at.%. The obtained results are relevant for achieving efficient laser operation of Tm^{3+}:CaF_2 crystals at the $^3F_4 \rightarrow {}^3H_6$ (at ~1.9 μm) and the $^3H_4 \rightarrow {}^3H_5$ (at ~2.3 μm) transitions.

Keywords: calcium fluoride, thulium ions, cross-relaxation, ion clustering, luminescence.

1. INTRODUCTION

Cubic (fluorite-type) calcium fluoride (CaF_2) crystals are well-known for fabrication of optical elements because of their good thermo-mechanical properties (thermal conductivity: κ ~9.7 W/(mK) for an undoped crystal), broad transparency range (0.13–10 μm) and low refractive index (n = 1.424 at ~2 μm). CaF_2 crystals are also suitable for doping with trivalent rare-earth ions (RE^{3+}) for laser applications [1-3]. They feature a strong RE^{3+} ion clustering even at low doping concentrations about 0.1–1 at.% [4,5] resulting in broad and smooth spectral bands both in absorption and emission (the so-called glassy-like spectroscopic behavior). It is of interest for broadly tunable [6] and mode-locked [7,8] lasers. The good thermal properties of the host matrix allow for power scaling.

Thulium (Tm^{3+}) doped CaF_2 crystals exhibit a broadband emission at ~1.9 μm due to the $^3F_4 \rightarrow {}^3H_6$ electronic transition. Efficient Tm^{3+}:CaF_2 lasers were reported [2,9]. Camy *et al.* reported on a laser-pumped Tm:CaF_2 laser delivering ~135 mW at 1887 nm with a slope efficiency of 41% and a laser threshold of only 68 mW [2]. Liu *et al.* reported on power scaling of a Tm:CaF_2 laser under diode-pumping yielding 2.71 W with a higher slope efficiency of 70.1% [9]. The same group of authors demonstrated continuous wavelength tunability for this laser between 1.85 and 2.04 μm (189 nm broad) and mode-locked operation employing a SESAM. In the latter case, 15 ps-long pulses were obtained at a central wavelength of 1886.8 nm with a repetition rate of 96.35 MHz [9]. Thin films of Tm:CaF2 were grown [10].

It was proven that the ion clustering determines the emission properties of Tm^{3+} ions in CaF_2 [5]. For low doping levels (0.01-0.1 at.%), the Tm^{3+} ions are mostly isolated and they accommodate in sites with different symmetry depending on the charge compensation mechanism involving interstitial F^- anions. For higher doping levels, ion clusters are formed. To prevent the clustering of active ions, the CaF_2 crystals were codoped by Tm^{3+} ions and optically passive "buffer" ions Ln^{3+} such as Gd^{3+}, Lu^{3+}, La^{3+} or Y^{3+} [11,12]. Laser operation with such codoped crystals was also demonstrated. Zhang *et al.* reported on a Tm,La:CaF_2 laser delivering 4.27 W at 1921 nm with a slope efficiency of 67.8% [12].

A key spectroscopic process which determines the laser efficiency of ~1.9 μm Tm lasers is the cross-relaxation (CR) for adjacent Tm^{3+} ions, $^3H_4(Tm_1) + {}^3H_6(Tm_2) \rightarrow {}^3F_4(Tm_1) + {}^3F_4(Tm_2)$, potentially leading to a pump quantum efficiency of 2 [13]. This means that after an excitation at ~0.8 μm (to the $^3H_4$ pump level), there can be up to 2 excited ions in the upper laser level ($^3F_4$). CR in Tm^{3+}-doped laser materials increases the laser slope efficiency and reduces the heat dissipation. Up to now, no detailed study of CR for Tm:CaF_2 crystals was performed.

*e-mail: pavel.loiko@ensicaen.fr

The aim of the present work is to study the cross-relaxation (and other energy-transfer processes, such as energy-transfer upconversion (ETU)) in Tm:CaF_2 crystals accounting for the ion clustering. For this, we involve the spectroscopic model of distinct ion classes which was recently developed [14].

2. EXPERIMENTAL RESULTS

For the spectroscopic studies, we grew a series of Tm^{3+}:CaF_2 crystals with the doping level ranging from 0.01 at.% to 7 at.%. The Tm:CaF_2 crystals were grown using a conventional Bridgman technique with a homemade furnace. A mixture of high purity (4N) CaF_2 and TmF_3 powders was introduced in a graphite crucible. A good vacuum ($<10^{-5}$ mbar) was realized before introducing Ar and CF_4 gases to avoid oxygen pollution. The furnace temperature was set to about 50 K higher than the melting point of CaF_2. After soaking, the charge was thoroughly melted and the crystal growth was carried out with a rate of 2-4 mm/h. When the growth was finished, the crystal was cooled down to room temperature (RT, 293 K) within 48 hours.

2.1 Absorption and luminescence

The RT absorption spectra of Tm^{3+}:CaF_2 crystals containing predominantly isolated ions (0.05 at.% Tm) and ion clusters (1.5 at.% and 4.5 at.% Tm) are shown in Fig. 1. It is known that in Tm^{3+}-doped CaF_2 crystals with very low doping levels, the active ions are distributed over three types of sites with the symmetry C_{3v} (trigonal), C_{4v} (tetragonal) or O_h (cubic). The particular symmetry depends on the charge compensation mechanism (as trivalent Tm^{3+} ions are replacing the divalent Ca^{2+} ones). The latter is provided by an interstitial fluorine anion (F_i^-). Here, we do not consider the possible charge compensation by oxygen (O^{2-}) or univalent alkali metal cations (Na^+, K^+) leading to other types of sites. As a result, the absorption spectra of the 0.05 at.% Tm^{3+}:CaF_2 crystal represent a superposition of sharp absorption lines of Tm^{3+} ions in all three sites. For high doping levels, the Tm^{3+} ions are mostly arranged in clusters leading to smooth and broad spectral bands. There is no significant change in the absorption spectra of 1.5 at.% Tm and 4.5 at.% Tm-doped crystals, except of the $^3H_6 \rightarrow {}^3H_5$ transition. The small changes may reflect the transition from simple clusters (dimers, trimers) to large agglomerates of active ions.

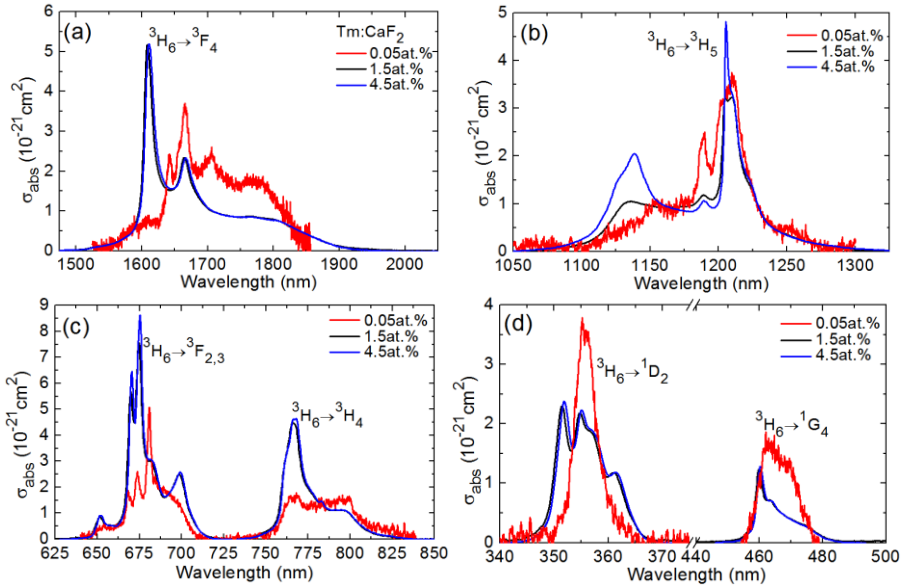

Figure 1. RT absorption cross-section, σ_{abs}, spectra of Tm^{3+}:CaF_2 crystals with different Tm doping concentrations (0.05 at.%, 1.5 at.% and 4.5 at.%): transitions from the ground-state ($^3H_6$) to the excited-states: (a) $^3F_4$, (b) $^3H_5$, (c) $^3H_4$ and $^3F_{2,3}$, and (d) $^1G_4$ and $^1D_2$.

For the $^3H_6 \rightarrow {}^3H_4$ pump transition, the maximum absorption cross-section σ_{abs} is 0.46×10^{-20} cm^2 at 766.2 nm and the full width at half maximum (FWHM) of the absorption band is 13.2 nm (for the 4.5 at.% Tm doping). For the 0.05 at.% Tm doping, the peak σ_{abs} value is much lower, 0.17×10^{-20} cm^2 at ~768 nm.

The evolution of RT luminescence spectra for the $^3H_4 \rightarrow {}^3H_6$ (at ~0.8 μm) and $^3F_4 \rightarrow {}^3H_6$ (at ~1.9 μm) transitions in emission was studied for a broad range of Tm doping concentrations (0.01–7 at.%). This comparative study revealed a critical Tm concentration (0.5–0.7 at.%) for which a significant change in the shape of the emission bands is observed: the spectra become smooth and broad and they resemble to a great extent those for Tm^{3+}-doped fluoride glasses. This is an indication of a change in the predominant ion coordination (a transition from isolated ions to clusters). Figure 2 shows such a comparison for the emission from the pump level ($^3H_4$) at ~0.8 μm.

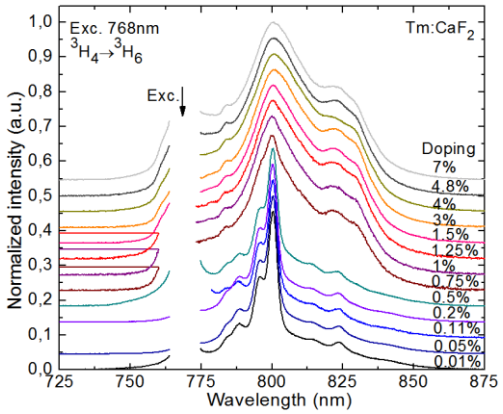

Figure 2. Normalized RT luminescence spectra of Tm^{3+}:CaF_2 crystals with different doping concentrations (the $^3H_4 \rightarrow {}^3H_6$ transition), λ_{exc} = 769 nm (non-selective excitation).

2.2 Luminescence decay

We monitored the decay of Tm^{3+} luminescence from the $^3H_4$ and $^3F_4$ multiplets for a broad range of Tm doping levels (0.01–7 at.%) in CaF_2. Figure 3 shows the measured luminescence decay curves for the $^3H_4 \rightarrow {}^3H_6$ transition in emission (at ~0.8 μm). For very low doping level (0.01 at.% Tm), the luminescence decay curve is close to a single-exponential one with a characteristic lifetime τ_{lum} of 3.55 ms. Despite the existence of several species contributing to this emission (namely, isolated Tm^{3+} ions in various sites), the intrinsic lifetimes of the $^3H_4$ state for the C_{3v} and C_{4v} coordinated Tm^{3+} ions in CaF_2 are rather close: 3.03 ms and 3.59 ms, respectively (as determined in site-selective excitation experiments). With increasing Tm doping, the decay from the $^3H_4$ state becomes faster and the luminescence decay curves notably deviate from the single-exponential law.

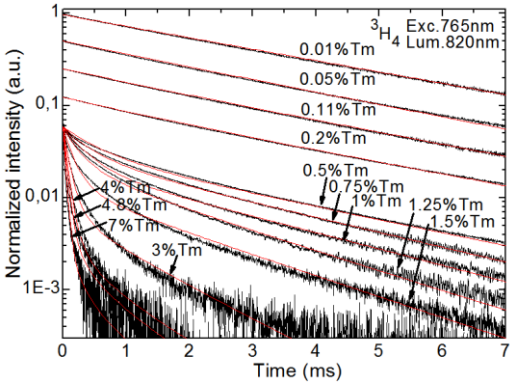

Figure 3. Luminescence decay curves from the $^3H_4$ Tm^{3+} state in Tm^{3+}:CaF_2: *black* – experimental data, *red* – their fitting with the rate-equation model of distinct ion classes, λ_{exc} = 765 nm, λ_{lum} = 820 nm. Measured under ns pulse excitation.

To explain this behavior, we used the model of spectroscopically distinct ion classes [14]. A simplified scheme of Tm^{3+} energy-levels was considered, Fig. 4. The populations of the Tm^{3+} ground-state ($^3H_6$) and two relevant excited-states ($^3F_4$ and $^3H_4$) were monitored; the population of the intermediate $^3H_5$ excited-state was assumed to be almost zero as this state is depopulated by very efficient multi-phonon non-radiative (NR) relaxation. The states above $^3H_4$ were not taken into account. The following spectroscopic processes were considered: (i) radiative (R) decay from the $^3F_4$ and $^3H_4$ states, (ii) cross-relaxation (CR) $^3H_4(Tm_1) + {}^3H_6(Tm_2) \rightarrow {}^3F_4(Tm_1) + {}^3F_4(Tm_2)$, (iii) energy-transfer upconversion, $^3F_4(Tm_1)$ +

$^3F_4(Tm_2) \rightarrow {}^3H_6(Tm_1) + {}^3H_4(Tm_2)$ (ETU_1) and $^3F_4(Tm_1) + {}^3F_4(Tm_2) \rightarrow {}^3H_6(Tm_1) + {}^3H_5(Tm_2)$ (ETU_2), and (iv) energy-migration (EM) to impurities leading to de-excitations from the $^3F_4$ and $^3H_4$ multiplets. We assumed the existence of two distinct ion classes: (a) isolated ions showing no energy-transfer processes (CR and ETU) and (b) ions with neighbors exhibiting both CR and ETU. The fraction of ions with neighbors f, the macroscopic rates of CR (W_{CR}) and ETU (W_{ETU1} and W_{ETU2}) and the $^3H_4$ level lifetime τ_3 accounting for EM were used as free parameters of the fitting (for luminescence decay curves shown in Fig. 3). The model gives a satisfactory agreement with the experiment.

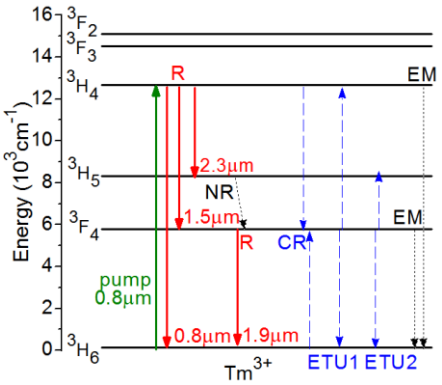

Figure 4. The scheme of energy-levels of Tm^{3+} ions (for a free-ion) showing relevant spectroscopic processes associated with the conventional pumping scheme (to the $^3H_4$ state): R – radiative relaxation, NR – multiphonon non-radiative relaxation, CR – cross-relaxation, ETU – energy-transfer upconversion, EM – energy-migration.

3. DISCUSSION

The results on the fraction of Tm^{3+} ions with neighbors f are shown in Fig. 5. With increasing the Tm doping level, the fraction of isolated ions ($1 - f$) gradually decreases. The critical Tm doping level for which at least half of the active ions are clustered is only 0.7±0.1 at.%. This agrees well with our conclusion drawn from the measured luminescence spectra at ~0.8 μm. The dependence of f on the doping concentration was fitted using a statistical approach [14,15]:

$$P_{m,n} = \frac{n!}{m!(n-m)!} p^m (1-p)^{n-m}. \quad (1)$$

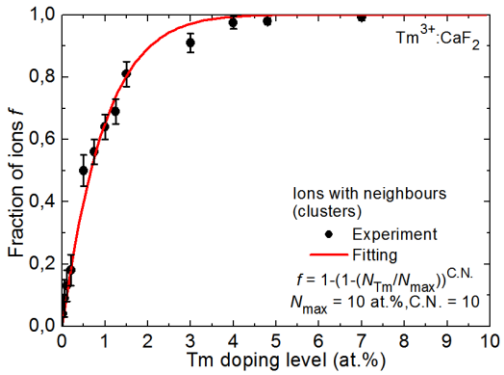

Figure 5. Ion clustering in Tm^{3+}:CaF_2: fraction of ions with neighbors f, *symbols* – data extracted from the modeling of the experimental luminescence decay curves using the rate-equation model of distinct ion classes, *curve* – their fit using a statistical approach.

Here, $P_{m,n}$ is the probability for occurrence of neighbor Tm^{3+} ions in the first coordination sphere of the considered Tm^{3+} ion, n is the coordination number (C.N.) by nearest-neighbor rare-earth sites, m is the actual number of Tm^{3+} ions in the first coordination sphere ($m = 0$ corresponds to a single ion and $m \geq 1$ - to an ion pair or cluster), and $p = N_{Tm}/N_{max}$ represents the relative doping concentration (N_{max} is the maximum possible concentration). The expression for the fraction of ions with neighbors ($m \geq 1$, not specifying the exact m number) is:

$$f = 1-[1-(N_{Tm}/N_{max})]^{C.N.}. \quad (2)$$

For calculation, we assume N_{max} = 10 at.% and C.N. = 10 which gives a good agreement with the data obtained from the measured luminescence curves.

The model also yields the macroscopic rates W_{CR}, W_{ETU1} and W_{ETU2} [in s^{-1}], as shown in Fig. 6. The CR is Tm:CaF_2 is much stronger than the ETU. W_{CR} and $W_{ETU1(2)}$ show a quadratic dependence on the Tm doping concentration (N_{Tm}):

$$W_{CR} = C_{CR} N_{Tm}^{\ 2}, \quad (3a)$$

$$W_{ETU1(2)} = C_{ETU1(2)} N_{Tm}^{\ 2}, \quad (3b)$$

where C_{CR} and $C_{ETU1(2)}$ are the concentration-independent microscopic energy-transfer parameters. CR in Tm^{3+}:CaF_2 is about one order of magnitude stronger than that in other well-known fluoride crystal, Tm^{3+}:$LiYF_4$ [16].

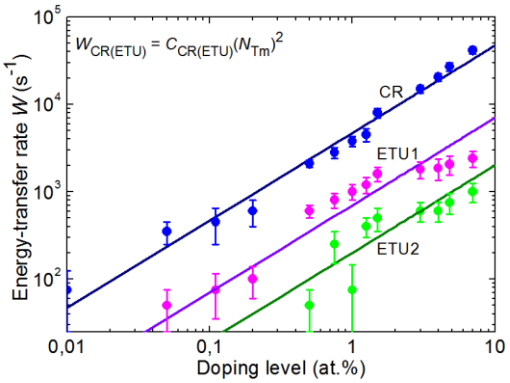

Figure 6. Energy-transfer processes in Tm^{3+}:CaF_2: macroscopic rates of cross-relaxation (CR) W_{CR} and energy-transfer upconverison (ETU) $W_{ETU1(2)}$, *symbols* – data extracted from the modeling of the experimental luminescence decay curves using the rate-equation model of distinct ion classes, *lines* – their quadratic fits.

4. CONCLUSIONS

To conclude, we have quantified ion clustering (in terms of fraction of ions with neighbors) and CR and ETU energy-transfer processes (in terms of macroscopic rates and microscopic concentration-independent parameters) in Tm^{3+}-doped CaF_2 crystals, for the first time, to the best of our knowledge. This information is of key importance for the design of Tm:CaF_2 lasers operating on the $^3F_4 \rightarrow {}^3H_6$ (~1.9 μm) and $^3H_4 \rightarrow {}^3H_5$ (~2.3 μm [17]) transitions. Indeed, for the ~1.9 μm lasers, quantification of CR is important to determine the possibility to reach high pump quantum efficiency of 2 for the upper laser level ($^3F_4$) [13]. For the ~2.3 μm lasers which have not been demonstrated yet in Tm:CaF_2, in contrast, CR is a detrimental effect as it quenches the lifetime of the upper laser level ($^3H_4$). However, ETU1 in such lasers can play a key role in refilling the $^3H_4$ state leading to increased laser slope efficiency [16,18]. The proposed spectroscopic model can be extended to describe the ion clustering in Tm^{3+},Ln^{3+}:CaF_2 crystals codoped with "buffer" ions.

5. ACKNOWLEDGEMENTS

This work was supported by the Agence Nationale de la Recherche (ANR), SPLENDID2 Project; European Community funds FEDER; Normandie region, NOVAMAT Project.

REFERENCES

[1] F. Druon, S. Ricaud, D. N. Papadopoulos, A. Pellegrina, P. Camy, J. L. Doualan, R. Moncorgé, A. Courjaud, E. Mottay, and P. Georges, "On Yb:CaF_2 and Yb:SrF_2: review of spectroscopic and thermal properties and their impact on femtosecond and high power laser performance," Opt. Mater. Express 1(3), 489–502 (2011).

[2] P. Camy, J.L. Doualan, S. Renard, A. Braud, V. Menard, and R. Moncorgé, "Tm^{3+}:CaF_2 for 1.9 μm laser operation," Opt. Commun. 236(4-6), 395-402 (2004).

[3] Labbe, C., Doualan, J.L., Camy, P., Moncorgé, R. and Thuau, M., "The 2.8 μm laser properties of Er^{3+} doped CaF_2 crystals," Opt. Commun. 209(1-3), 193-199 (2002).
[4] V. Petit, P. Camy, J.-L. Doualan, X. Portier, and R. Moncorgé, "Spectroscopy of Yb^{3+}:CaF_2: from isolated centers to clusters," Phys. Rev. B Condens. Matter Mater. Phys. 78(8), 085131 (2008).
[5] S. Renard, P. Camy, A. Braud, J. L. Doualan, and R. Moncorgé, "CaF_2 doped with Tm^{3+}: A cluster model," J. Alloys Compd. 451(1-2), 71-73 (2008).
[6] A. Lucca, M. Jacquemet, F. Druon, F. Balembois, P. Georges, P. Camy, J. L. Doualan, and R. Moncorgé, "High-power tunable diode-pumped Yb^{3+}:CaF_2 laser," Opt. Lett. 29(16), 1879–1881 (2004).
[7] A. Lucca, G. Debourg, M. Jacquemet, F. Druon, F. Balembois, P. Georges, P. Camy, J. L. Doualan, and R. Moncorgé, "High-power diode-pumped Yb^{3+}:CaF_2 femtosecond laser," Opt. Lett. 29(23), 2767–2769 (2004).
[8] Friebel, F., Druon, F., Boudeile, J., Papadopoulos, D.N., Hanna, M., Georges, P., Camy, P., Doualan, J.L., Benayad, A., Moncorgé, R. and Cassagne, C., "Diode-pumped 99 fs Yb:CaF_2 oscillator," Opt. Lett. 34(9), 1474-1476 (2009).
[9] Liu, J., Zhang, C., Zhang, Z., Wang, J., Fan, X., Liu, J. and Su, L., "1886-nm mode-locked and wavelength tunable Tm-doped CaF_2 lasers," Opt. Lett. 44(1), 134-137 (2019).
[10] Brasse, G., Loiko, P., Grygiel, C., Leprince, P., Benayad, A., Lemarie, F., Doualan, J.L., Braud, A. and Camy, P., "Liquid Phase Epitaxy growth of Tm^{3+}-doped CaF_2 thin-films based on LiF solvent," J. Alloys Compd. 803, 442-449 (2019).
[11] X. Liu, K. Yang, S. Zhao, T. Li, C. Luan, X. Guo, B. Zhao, L. Zheng, L. Su, J. Xu, and J. Bian, "Growth and lasing performance of a Tm,Y:CaF_2 crystal," Opt. Lett. 42(13), 2567-2570 (2017).
[12] Zhang, Z., Guo, X., Wang, J., Zhang, C., Liu, J. and Su, L., "High-efficiency 2 μm continuous-wave laser in laser diode-pumped Tm^{3+},La^{3+}:CaF_2 single crystal," Opt. Lett. 43(17), 4300-4303 (2018).
[13] K. van Dalfsen, S. Aravazhi, C. Grivas, S. M. García-Blanco, and M. Pollnau, "Thulium channel waveguide laser with 1.6 W of output power and ~80% slope efficiency," Opt. Lett. 39(15), 4380-4383 (2014).
[14] P. Loiko, and M. Pollnau, "Stochastic model of energy-transfer processes among rare-earth ions. Example of Al_2O_3:Tm^{3+}," J. Phys. Chem. C 120(46), 26480-26489 (2016).
[15] Voron'ko, Y.K., Mamedov, T.G., Osiko, V.V., Timoshechkin, M.I. and Shcherbakov, I.A., "Effect of donor-donor and donor-acceptor interactions on the decay kinetics of the metastable state of Nd^{3+} in crystals," Sov. J. Exp. Theor. Phys. 38, 565 (1974).
[16] Loiko P., Soulard R., Guillemot L., Brasse G., Doualan J.L., Braud A., Tyazhev A., Hideur A., Druon F., and Camy P., "Efficient Tm:$LiYF_4$ lasers at 2.3 μm: Effect of energy-transfer upconversion," IEEE J. Quantum Electron. 55(6), 1700212 (2019).
[17] Pinto J. F., Esterowitz L., and Rosenblatt G. H., "Tm^{3+}:YLF laser continuously tunable between 2.20 and 2.46 μm," Opt. Lett. 19(12), 883-885 (1994).
[18] Guillemot L., Loiko P., Soulard R., Braud A., Doualan J.L., Hideur A., and Camy P., "Close look on cubic Tm:KY_3F_{10} crystal for highly efficient lasing on the $^3H_4 \rightarrow {}^3H_5$ transition," Opt. Express 28(3), 3451-3463 (2020).